

Separability of Input Features and the Resulting Accuracy in Classifying Target Poses for Active Transhumeral Prosthetic Interfaces

Tianshi Yu, Ricardo Garcia-Rosas, Alireza Mohammadi, Ying Tan, Peter Choong and Denny Oetomo

Abstract—In active prostheses, it is desired to achieve target poses for a given family of tasks, for example, in the task of forward reaching using a transhumeral prosthesis with coordinated joint movements. To do so, it is necessary to distinguish these target poses accurately using the input features (e.g. kinematic and sEMG) obtained from the human users. However, the input features have conventionally been selected through human observations and influenced heavily by the availability of sensors in this context, which may not always yield the most relevant information to differentiate the target poses in the given task. In order to better select from a pool of available input features, those most appropriate for a given set of target poses, a measure that correlates well with the resulting classification accuracy is required so that it can inform the interface design process. In this paper, a scatter-matrix based class separability measure is adopted to quantitatively evaluate the separability of the target poses from their corresponding input features. A human experiment was performed on ten able-bodied subjects. Subjects were asked to perform forward-reaching movements with their arms on nine target poses in a virtual reality (VR) platform and the corresponding kinematic information of their arm movement and muscle activities were recorded. The accuracy of the prosthetic interface in determining the intended target poses of the human user during forward reaching is evaluated for different combinations of input features, selected from the kinematic and sEMG sensors worn by the users. The results demonstrate that employing input features that yield a high separability measure between target poses results in a high accuracy in identifying the intended target poses in the execution of the task.

I. INTRODUCTION

Active transhumeral (TH) prostheses, unlike transradial (TR) ones [1], which are mainly used to perform fine motor tasks such as object grasping, are also used to perform gross motor tasks such as forward reaching with a target pose. By active, we refer to motorised prostheses, where input signals measured by worn sensors are processed through a prosthetic interface to inform the intended prosthesis movements. TH prosthetic interfaces that can generate coordinated motion between residual limb and prosthesis have recently gained much attention. Recent work in [2] has validated that such interfaces can be more efficient and intuitive in performing reaching tasks than traditional two-site surface electromyography (sEMG) interface and is preferred by users [3].

For the task of reaching the target poses, it is necessary for the interface to be able to distinguish accurately the intended

poses by the human user. Some input features naturally contain less distinguishing information content to particular target poses than others. For example, in the case of a transhumeral amputees, a set of kinematic sensors measuring the joint angles of the residual shoulder would be a poor predictor to what the users intend to do with their prosthetic elbow [4]. In such a scenario, there are multiple possible target poses that share the same shoulder joint angles, but different amount of intended elbow flexion. It is therefore important to consider the information content of the available input features in order to select those most appropriate for the given target poses that we require the prosthetic interface to distinguish.

Existing active TH prosthetic interfaces in the literature have reported trial-and-error methods or designer-observational approaches when designing the input features. The choices of sensors also often depend on the conveniently available sensors for the application. The common practice [2], [5]–[7] is that kinematic features extracted from residual limb and body kinematics were chosen based on different observation of human motor behaviours. Shoulder rotation features were the most commonly used [2], [5] according to the study on upper-extremity joint coordination [8], [9]. In [6], scapular translational movement features were added, as the corresponding movement was observed during the forward reaching to the proximal end. In recent years, the combined use of kinematics and muscle activity sensors (sEMG) have been considered [10]–[12]. Naturally, this provides access to a wider range of input information, bringing the potential for more accurate identification of the human user intention. In [10], 28 sEMG features from seven electrodes and three shoulder kinematics features were used altogether. While such setup is suited for a laboratory experiment, the need for such numerous number of sensors may not be practical for daily usage. It is necessary to identify the most useful input features for the intended target poses.

In order to select the appropriate input features, it is necessary for a quantitative surrogate measure to be established, which correlates well with the resulting accuracy of the selected input features in differentiating the target poses needed in a given task. In this work, the concept of class-separability and a widely-used scatter-matrix based measure [13] are adopted to quantitatively evaluate the separability of the target poses as described by input features selected from the available pool. The task is limited herein to forward reaching motion, with target poses similar to [6], [10] used for the purpose of classification. Three common feature

This project is funded by the Valma Angliss Trust and The University of Melbourne.

T. Yu, R. Garcia-Rosas, D. Oetomo, and Y. Tan are with the School of Electrical, Mechanical and Infrastructure Engineering, and P. Choong with the Department of Surgery, The University of Melbourne, VIC 3010, Australia. {tianshiy}@student.unimelb.edu.au; {garcia.r,alireza.mohammadi,yingt.pchoong,doetomo}@unimelb.edu.au.

modality cases in prosthetic context are investigated: (1) using kinematic features only [14], (2) using sEMG features only [15] and (3) combining kinematic and sEMG features [10]. Data were collected from a human-subject experiment in a virtual reality (VR) environment. The experiments were performed on ten able-bodied subjects for a forward reaching task on nine target poses. An extensively used classifier based on linear discriminant analysis (LDA) was trained using the collected data [16], [17]. The resulting classification accuracy of the prosthetic interface using a set of input features is compared to the corresponding separability measures.

II. METHODOLOGY

The experiment and the methodology of the study is described below.

A. Target pose separability

Class separability is widely used to evaluate the input features in a classification problem. Scatter-matrix based measurement [13] is adopted in this paper for its simplicity and generality. Let F be the set containing D candidate features, $F = \{f_1, \dots, f_D\}$. The target pose set is denoted as P with C target classes with $P = \{T_1, \dots, T_C\}$.

The sampled data matrix $\mathbf{X} = [\mathbf{x}_1, \dots, \mathbf{x}_n] \in \mathbb{R}^{d \times n}$ contains n samples of the d selected features in some set $F_s \subseteq F$. Each sample \mathbf{x}_i ($i = 1, \dots, n$) is assigned to a label with c classes in some target subset $P_s \subseteq P$ that is of interest. Let n_j be the number of samples in the j^{th} class, i.e., $\sum_{j=1}^c n_j = n$. Then, by using an appropriate relabeling of n samples, denote $\mathbf{x}_{j,k}$ ($j = 1, \dots, c, k = 1, \dots, n_j$) to represent the k^{th} samples of the j^{th} class. The inter-class and intra-class scatter matrix \mathbf{S}_B and \mathbf{S}_W are

$$\mathbf{S}_B = \sum_{j=1}^c n_j (\mathbf{m}_j - \mathbf{m})(\mathbf{m}_j - \mathbf{m})^T, \quad (1)$$

$$\mathbf{S}_W = \sum_{j=1}^c \sum_{k=1}^{n_j} (\mathbf{x}_{j,k} - \mathbf{m}_j)(\mathbf{x}_{j,k} - \mathbf{m}_j)^T, \quad (2)$$

where $\mathbf{m}_j \in \mathbb{R}^d$ is the mean of the j^{th} class, computed from the sampled data in the j^{th} class while $\mathbf{m} \in \mathbb{R}^d$ is the mean of all samples. Finally, the target pose separability s provided by any features set F_s for any class set of P_s , is evaluated by ratio trace of \mathbf{S}_B and \mathbf{S}_W

$$s = \text{tr}(\mathbf{S}_W^{-1} \mathbf{S}_B) \text{ if } \det(\mathbf{S}_W) \neq 0, \quad (3)$$

where $\det(\cdot)$ is the determinant of a square matrix. The separability measure s is always positive. Note that the higher the s , the better the separability and vice versa. The determinant $\det(\mathbf{S}_W)$ is zero only if at least one of the features is a linear combination of the other features, which is unlikely due to human movement variability.

B. Experiment description and protocol

A human experiment with ten able-bodied subjects was conducted in VR environment to record a set of kinematic and sEMG input features associated with the human subject arm and upper body movements reaching for target poses

placed along the parasagittal plane of extending upper limb forward. The procedure was approved by the University of Melbourne Human Research Ethics Committee, project ID 11878. Informed consent was received from all subjects. Subjects were asked to perform forward reaching task towards nine target poses, marked in the head mounted display based VR environment, for ten iterations each, see Fig. 1(a). The final reaching poses were held for one second to allow the quasi-static readings upon reaching to be collected.

Nine target poses (T1-T9) set in the parasagittal plane were set based on the joint space human arm displacements, as illustrated in Fig. 1(b). To set the locations of the targets, subjects were required to reach the target joint poses as shown in Fig. 1(b) during the initialisation of the experiment. The set contained three groups of targets, namely target 1-3 (T1,T2,T3), target 4-6 (T4,T5,T6) and target 7-9 (T7,T8,T9). Targets in the same group have the same shoulder flexion/extension pose, but different elbow poses such that the target poses are indistinguishable from observing only the primary kinematic feature (shoulder flexion/extension). It should be noted that alternatively one can consider the prosthetic poses (e.g. elbow flexion/extension poses) as the target poses instead of the whole upper limb poses if only the prosthetic poses are of interest.

C. Data collection and preprocessing

Signals from kinematic and sEMG wearable sensors were collected, namely body and arm posture and sEMG. The data sampling rates were 90 and 1111 Hz, respectively. The sensor deployment is shown in Fig. 1(a). Three HTC VIVE Trackers with motion capture sensors on the surface and an embedded Inertial Measurement Unit (IMU) were attached to the subjects' upper-arm, shoulder acromion and C7 vertebrae to acquire upper-body and upper-arm postural data. Another tracker on the forearm and the controller in hand were utilised to control the arm in VR environment only. Despite the usage of both motion capture and IMUs for kinematic data collection herein, this can also be achieved using IMU-only as in [5]. Seven Delsys Trigno sEMG electrodes were placed on the dominant upper-arm of the subjects: two on the biceps long/short heads (B-LH/B-SH), two on the triceps lateral/long heads (T-LAH/T-LH), three on the anterior, middle and posterior of deltoid (D-A/D-M/D-P). The signals were filtered by a 4th order Butterworth band-pass filter with 10-500 Hz passband. Then the outliers which

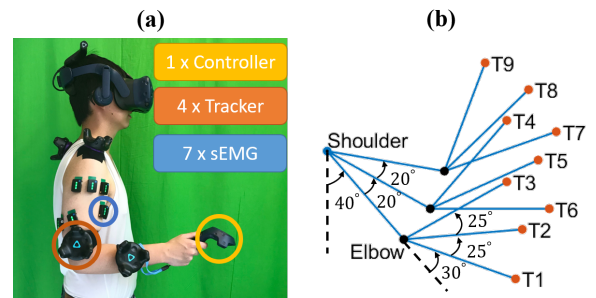


Fig. 1. (a) Experiment setup and sensor deployment, (b) Target set with target poses within the sagittal plane, T1-T9 denote the target poses.

were more than three standard deviations from the mean were removed.

D. Feature extraction

The candidate features were extracted from the quasi-static data during the last-second holding period upon reaching the target poses in a coordinated fashion. For each of the seven signal sites of sEMG, a sliding window of length 200ms overlapping 100ms (resulting 10Hz sampling rate) was used to extract four time domain features: mean absolute value (MAV), wave length (WL), zero crossing (ZC), slope change (SC) as defined in [16]. Kinematic posture data were downsampled to 10Hz as well. The kinematic features are: shoulder flexion/extension (Sfe) and abduction/adduction (Saa); shoulder scapular depression/elevation (Scde) and protraction/retraction (Scpr); and trunk flexion/extension (Tfe) and left/right bending (Tb). Since the targets were in the parasagittal plane, shoulder internal/external rotation and trunk rotation was not considered. In total, $D = 34$ features were extracted as the candidates and were normalised to zero-mean and unit-variance for each subject. The motion trajectory of position, velocity and acceleration were not considered.

E. Evaluation of kinematic and sEMG features

Three common scenarios of feature modality in prosthetic interface context are investigated herein, which are (1) kinematic-only, (2) sEMG-only and (3) kinematic-sEMG features (combined). In this paper, we chose to evaluate the performance of the resulting prosthesis interface using only two input features. This was selected to keep a low complexity not only for the resulting interface, but also to

maintain the focus on the discussion in this paper and to keep a fair comparison in the number of features in this short paper. The two features ($d = 2$) with the highest separability for the interested target pose set $P_s = \{T1-T9\}$ (P_s will be omitted for simplicity henceforth) was selected through brute-force evaluation of all combinations of input features. An LDA based classifier was trained to test the accuracy of the selected input features in distinguishing the target poses, where the training set (60%, six iterations) and testing set (40%, four iterations) were split randomly for each target pose.

III. RESULTS AND DISCUSSION

Brute-force evaluation of separability measure for all combination of input feature pairs yielded the following selections: (1) Sfe, Scpr for kinematic-only (2) B-LH (MAV), D-M (SC) for sEMG-only and (3) Sfe, B-LH (MAV) for combined kinematic-sEMG.

Fig. 2(a) shows the separability of all the pair-wise combinations of target poses (numbered 1 to 9), using input features from kinematic only sensors, sEMG only sensors and the combined kinematic-sEMG sensors. Darker and lighter colours represent lower and higher separability, respectively. Black diagonal entries mean zero separability for target poses from the same class (the same target poses). Ideally, all off-diagonal entries should be white, meaning all target poses i should be separable from target pose j , where $i \neq j$.

Fig. 2(b) shows the accuracy of the classification results for the corresponding cases (kinematics, sEMG, combined kinematic-sEMG) in the form of confusion matrices. A high degree of correlation can be observed visually between

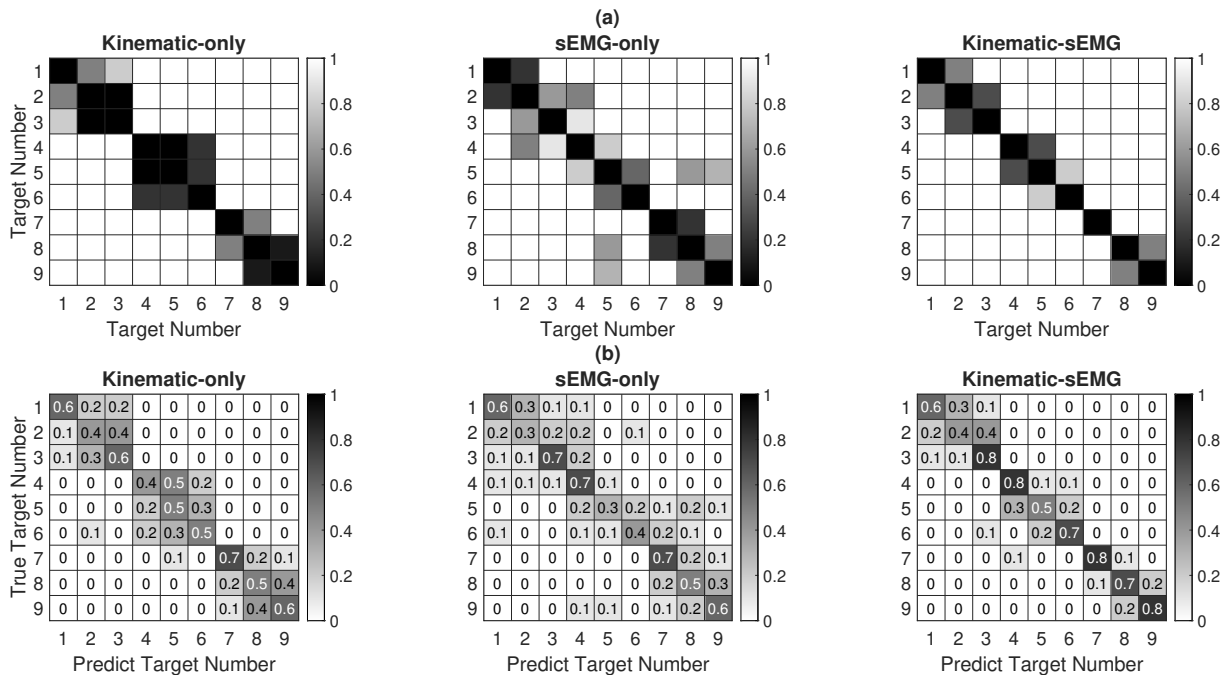


Fig. 2. Fig. (a) shows the heatmap of the class separability measures for the combined results of all subjects, with input features selected from kinematic-sensor-based features, sEMG-sensor-based features and combined kinematic and sEMG features. Darker and lighter colours show lower and higher separability, respectively. Fig. (b) shows the resulting accuracy of the corresponding prosthesis interface, represented by a confusion matrix of classification results using the same input feature pair.

TABLE I
MEAN & MINIMUM SEPARABILITY BETWEEN CLASSES AND
CLASSIFICATION ACCURACY PERCENTAGE FOR THREE MODALITY CASES

Item	kinematic-only	sEMG-only	kinematic-sEMG
	Separability (s)		
Mean-s	9.93	2.45	9.68
Min-s	0.02	0.20	0.31
	Classification Accuracy (%)		
Group	52.22	51.67	68.06
S1	44.44	58.33	83.33
S2	55.56	72.22	80.56
S3	50.00	44.44	61.11
S4	66.67	41.67	50.00
S5	38.89	41.67	58.33
S6	69.44	52.78	77.78
S7	61.11	69.44	91.67
S8	38.89	50.00	75.00
S9	44.44	38.89	50.00
S10	52.78	47.22	52.78

the separability (Fig. 2(a)) and the resulting accuracy (Fig. 2(b)), where entries with lower separability result in lower classification accuracy.

Quantitatively, the average and minimum separability measures between two target poses were calculated and shown in Tab. I (in the first two rows). The Tab. I also shows the classification accuracy for each subject (and the group) under three different modalities of the input features.

A significant difference of mean separability ($p < 0.01$ using two-way ANOVA) was found between sEMG-only and kinematic-sEMG, and the latter had both higher separability and classification accuracy. Though no significant difference in mean separability was found between kinematic-only and kinematic-sEMG, the minimum value was improved significantly in the kinematic-sEMG case. The kinematic-sEMG case, where the input feature selection can be made out of a wider range of input sensor modalities, showed a significantly higher separability between any two target poses, resulting in higher classification accuracy being observed over the group results and most subjects, except in Subject S4.

As an additional observation, it can be seen from Fig. 2 and Tab. I that having access to both the kinematics and sEMG modality of sensors improved the classification accuracy, which agree with the findings in [10]. As expected, the kinematic features performed well differentiating target poses in different shoulder poses, but performed poorly in differentiating targets with common shoulder poses (e.g. {T1-T3}, {T4-T6} and {T7-T9}). This was equally picked up by the separability measures as shown in Fig. 2(a). When used in isolation, the sEMG did not produce any better separability nor accuracy relative to kinematics-only features. However, it significantly assisted in distinguishing the target poses with common shoulder angles, which was confounding the outcomes of the kinematic features.

IV. CONCLUSION

The separability measure, proposed here for adoption to the problem of prosthetic interface input feature evaluation, is shown to be a valid surrogate measure of the accuracy

in classifying the target poses and to determine the N most effective features. The classification results also indicates the need for systematically selecting a larger input feature subset from the available sensor information. It is worth noting that the selection needs to trade off efficacy and complexity. A small number of sensors is preferred on wearable devices as in [17] to reduce the complexity. Meanwhile, sufficient separability should be retained for efficacy. Future work will investigate the use of this measure in an optimisation exercise to determine an optimal set of input features for a given set of target poses.

REFERENCES

- [1] A. Mohammadi *et al.*, "A practical 3d-printed soft robotic prosthetic hand with multi-articulating capabilities," *PLoS one*, vol. 15, no. 5, p. e0232766, 2020.
- [2] M. Merad *et al.*, "Assessment of an automatic prosthetic elbow control strategy using residual limb motion for transhumeral amputated individuals with socket or osseointegrated prostheses," *IEEE Trans. Med. Robot. Bionics.*, vol. 2, no. 1, pp. 1–1, 2020.
- [3] F. Cordella *et al.*, "Literature review on needs of upper limb prosthesis users," *Front. Neurosci.*, vol. 10, p. 209, 2016.
- [4] R. Garcia-Rosas, D. Oetomo, C. Manzie, Y. Tan, and P. Choong, "Task-space Synergies for Reaching using Upper-limb Prostheses," *IEEE Trans. Neural Syst. Rehabil. Eng.*, vol. 28, no. 12, pp. 2966–2977, 2020.
- [5] R. Garcia-Rosas, T. Yu, D. Oetomo, C. Manzie, Y. Tan, and P. Choong, "Exploiting inherent human motor behaviour in the online personalisation of human-prosthetic interfaces," *IEEE Robot. Autom. Lett.*, vol. 6, no. 2, pp. 1973–1980, 2021.
- [6] R. R. Kaliki, R. Davoodi, and G. E. Loeb, "Evaluation of a noninvasive command scheme for upper-limb prostheses in a virtual reality reach and grasp task," *IEEE Trans. Biomed. Eng.*, vol. 60, no. 3, pp. 792–802, 2013.
- [7] M. Legrand, N. Jarrassé, F. Richer, and G. Morel, "A closed-loop and ergonomic control for prosthetic wrist rotation," in *IEEE Int'l Conf Rob & Autom.*, pp. 2763–2769, 2020.
- [8] G. Averta *et al.*, "On the time-invariance properties of upper limb synergies," *IEEE Trans. Neural Syst. Rehabil. Eng.*, vol. 27, no. 7, pp. 1397–1406, 2019.
- [9] T. R. Kaminski, C. Bock, and A. M. Gentile, "The coordination between trunk and arm motion during pointing movements," *Exp. Brain Res.*, vol. 106, no. 3, pp. 457–466, 1995.
- [10] A. Akhtar, N. Aghasadeghi, L. Hargrove, and T. Bretl, "Estimation of distal arm joint angles from EMG and shoulder orientation for transhumeral prostheses," *J. Electromyogr. Kinesiol.*, vol. 35, pp. 86–94, 2017.
- [11] D. Blana, T. Kyriacou, J. M. Lambrecht, and E. K. Chadwick, "Feasibility of using combined EMG and kinematic signals for prosthesis control: A simulation study using a virtual reality environment," *J. Electromyogr. Kinesiol.*, vol. 29, pp. 21–27, 2016.
- [12] N. A. Alshammary, D. A. Bennett, and M. Goldfarb, "Synergistic elbow control for a myoelectric transhumeral prosthesis," *IEEE Trans. Neural Syst. Rehabil. Eng.*, vol. 26, no. 2, pp. 468–476, 2018.
- [13] K. Fukunaga, *Introduction to statistical pattern recognition*. Computer science and scientific computing. Academic Press, 1990.
- [14] R. Garcia-Rosas, Y. Tan, D. Oetomo, C. Manzie, and P. Choong, "Personalized Online Adaptation of Kinematic Synergies for Human-Prosthesis Interfaces," *IEEE Trans. Cybern.*, vol. 51, no. 2, pp. 1070–1084, 2021.
- [15] R. M. Mayer *et al.*, "Tactile Feedback in Closed-Loop Control of Myoelectric Hand Grasping: Conveying Information of Multiple Sensors Simultaneously via a Single Feedback Channel," *Front. Neurosci.*, vol. 14, no. April, pp. 1–12, 2020.
- [16] A. Phinyomark, P. Phukpattaranont, and C. Limsakul, "Feature reduction and selection for EMG signal classification," *Expert Syst. Appl.*, vol. 39, no. 8, pp. 7420–7431, 2012.
- [17] A. Krasoulis, S. Vijayakumar, and K. Nazarpour, "Multi-grip classification-based prosthesis control with two EMG-IMU sensors," *IEEE Trans. Neural Syst. Rehabil. Eng.*, vol. 28, no. 2, pp. 508–518, 2019.